[10]G. W. Hoffman and W. R. Cohen, Phys. Rev. Letters 29, 22 (1972).
[11]R. St. Onge, T. Amos, A. Galonsky, and R. Jolly, Bull. Am. Phys. Soc. 15, 1671 (1970); 16, 1172 (1971).
[12]R. J. Kurz, Lawrence Radiation Laboratory Report No. UCRL 11339, March 1964 (unpublished).
[13]J. B. Hunt, C. A. Baker, C. J. Batty, P. Ford, E. Freidman, and L. E. Williams, Nucl. Instr. Methods 85, 269 (1970).
[14]J. D. Anderson, Bull. Am. Phys. Soc. 17, 527 (1972); and private communication.
[15]R. H. Bassel, R. M. Drisko, and G. R. Satchler, Oak Ridge National Laboratory Report No. 3240 (unpublished), and a subsequent memorandum to users of JULIE 1966 (unpublished).
[16]P. D. Kunz, private communication.
[17]G. R. Satchler, R. M. Drisko, and R. H. Bassel, Phys. Rev. 136, B637 (1964).
[18]A. M. Lane, Nucl. Phys. 35, 676 (1962).
[19]F. D Becchetti, Jr., and G. W. Greenlees, Phys. Rev. 182, 1190 (1969).
[20]F. G. Perey, Phys. Rev. 131, 745 (1963).
[21]F. Perey and B. Buck, Nucl. Phys. 32, 353 (1962).
[22]M. P. Fricke, E. E. Gross, B. J. Morton, and A. Zuker, Phys. Rev. 156, 1207 (1967).
[23]J. D. Carlson, D. A. Lind, and C. D. Zafiratos, to be published.
[24]W. L. Fadner, J. J. Kraushaar, and S. I. Hayakawa, Phys. Rev. C 5, 859 (1972).
[25]R. A. Hinrichs and D. A. Show, Phys. Rev. C 6, 1257 (1972).
[26]N. Thurlow, Nucl. Phys. A109, 471 (1968).

PHYSICAL REVIEW C VOLUME 7, NUMBER 5 MAY 1973

Properties of the Argon Isotopes*

D. H. Gloeckner, R. D. Lawson, and F. J. D. Serduke
Argonne National Laboratory, Argonne, Illinois 60439
(Received 22 January 1973)

The properties of the low-lying states of the argon isotopes $^{39}_{18}Ar_{21}$, $^{40}_{18}Ar_{22}$, $^{41}_{18}Ar_{23}$, and $^{42}_{18}Ar_{24}$ are predicted by use of both the $(\pi d_{3/2})^{-2}(\nu f_{7/2})^n$ model and the extended $(\pi d_{3/2})^{-2}(\nu f_{7/2}, \nu p_{3/2})^n$ description. The n-n, p-p, and n-p interactions are taken from data on neighboring nuclei. With the extended model, reasonable agreement with experiment is obtained for the spectra. $E2$ and $M1$ transitions rates are examined. All $M1$ transitions are predicted to be substantially inhibited, as is observed experimentally. Several experiments are suggested.

I. INTRODUCTION

In the past year several groups[1-5] have studied the properties of the even-mass $^{N+18}_{18}Ar_N$ nuclei with $N>20$ and much new data concerning the nuclei $^{40}_{18}Ar_{22}$ and $^{42}_{18}Ar_{24}$ have emerged. We have attempted to correlate this collection of data with the simple shell model in which two proton holes are restricted to the $d_{3/2}$ single-particle orbit and the neutrons are constrained either to the $f_{7/2}$ level or to the $f_{7/2}$ and $p_{3/2}$ levels.

Several investigators have attempted to understand the properties of specific argon isotopes. The properties of $^{39}_{18}Ar_{21}$ were studied by Maripuu and Hokken,[6] who used a modified surface δ parametrization of the residual two-body interaction. Calculations[7,8] using matrix elements of the Hamada-Johnston potential and of the Tabakin potential have been used to examine the properties of $^{40}_{18}Ar_{22}$. In those calculations, an attempt was made to calculate the matrix elements of the residual two-body interaction from a potential. In contrast, Shadmi and Talmi[9] determined the matrix elements of the residual interaction empirically. They were able to account for the large number of $l_n=1$ stripping states observed in $^{41}_{18}Ar_{23}$.

Our approach parallels that of Shadmi and Talmi. In Sec. II we discuss states whose wave functions have significant components outside the $(\pi d_{3/2})^{-2}(\nu f_{7/2}, \nu p_{3/2})^{N-20}$ model space. Section III is a discussion of the models we shall use in attempting to correlate the data on ^{39}Ar, ^{40}Ar, ^{41}Ar, and ^{42}Ar. Also, we describe the data that were fitted in our determination of the matrix elements of the residual interaction. Section IV compares our theoretical predictions with experimental results for these nuclei and suggests several experiments that may help to improve our understanding of these nuclides.

II. CORE-EXCITED STATES IN ARGON

Shell closure at $Z=20$, $N=20$ is not excellent. The second excited state, a 0^+ level, in $^{42}_{20}Ca_{22}$, $^{44}_{20}Ca_{24}$, and $^{46}_{20}Ca_{26}$ is known to have appreciable components outside the (fp) model space[10]; the first excited state in $^{43}_{21}Sc_{22}$, $^{45}_{21}Sc_{24}$, and $^{47}_{21}Sc_{26}$ is

a $\frac{3}{2}^+$ core-excited state.

In this section, we estimate the positions of the lowest-lying core-excited 0^+ states of $^{38}_{18}Ar_{20}$, $^{40}_{18}Ar_{22}$, and $^{42}_{18}Ar_{24}$. A previous calculation[11] that used only the experimental energies of the $\frac{3}{2}^+$ hole states in the scandium isotopes and known ground-state binding energies predicted that the $(\pi d_{3/2})^{-2}$ 0^+ hole state should lie at nearly the observed energy of the first excited 0^+ level in each of the even-A calcium isotopes. Here, the argon 0^+ core-excited states will be estimated from known binding energies and the observed positions of the lowest $\frac{3}{2}^+$ core-excited states in $^{39}_{18}Ar_{21}$, $^{41}_{18}Ar_{23}$, and the $\frac{7}{2}^-$ core-excited state in $^{37}_{18}Ar_{19}$.

The 0^+ core-excited states will be assumed to arise from the promotion of $d_{3/2}$ nucleons to the $f_{7/2}$ level. If we consider only configurations in which either the $d_{3/2}$ holes or the $f_{7/2}$ particles couple to zero angular momentum, the interaction energy of such a configuration may be written[11, 12] as

$$E_{df} = aN_d N_f + b\vec{T}_d \cdot \vec{T}_f ,$$
$$= aN_d N_f + \tfrac{1}{2}b[T(T+1) - T_d(T_d+1) - T_f(T_f+1)], \quad (1)$$

where N_d is the number of d holes, N_f is the number of f particles, T_d and T_f are the isospins of the d holes and the f particles, respectively, and T is the total isospin.

Consider $^{40}_{18}Ar_{22}$. In our simple model, its ground-state configuration is

$$\psi(\text{g.s.}, 0^+) = [{d_{01}}^{-2} \times {f_{01}}^2]_{02} , \quad (2)$$

where ${d_{01}}^{-2}$ is the state in which two $d_{3/2}$ holes couple to $J_d = 0$, $T_d = 1$ (i.e., the ^{38}Ar ground state) and ${f_{01}}^2$ is the neutron configuration of ^{42}Ca. The vector-coupling symbol $[\times]_{JT}$ implies that the spins and isospins of the constituents couple to a total angular momentum J and isospin T. The configuration of the core-excited 0^+ state in ^{40}Ar is

$$\psi(0^+{}^*) = [{d_{00}}^{-4} \times {f_{02}}^4]_{02} . \quad (3)$$

The energy of this configuration relative to that of the ground state is

$$E_{0^+{}^*} - E_{0^+} = W(\nu f^4)_{02} + W[\pi d^{-2} \times \nu d^{-2}]_{00} - W(\nu f^2)_{01} - W(\pi d^{-2})_{01} + 2\{\epsilon_{f\nu} + {\epsilon_{d\nu}}^{-1} + 6a - \tfrac{1}{2}b\}, \quad (4)$$

where $\epsilon_{f\nu}$ is the single-particle energy of an $f_{7/2}$ neutron and ${\epsilon_{d\nu}}^{-1}$ is the single-hole energy of a $d_{3/2}$ neutron, both referred to the ^{40}Ca core, and the W's are interaction energies. For example, $W(\nu f^4)_{J=0,\,T=2}$ is the interaction energy of four $f_{7/2}$ neutrons coupling to $J=0$, $T=2$ and its value is determined from the mass tables[13] by subtracting four $f_{7/2}$ neutron single-particle energies from the binding energy of ^{44}Ca.

The only undetermined quantity in Eq. (4) is $\{\epsilon_{f\nu} + {\epsilon_{d\nu}}^{-1} + 6a - \frac{1}{2}b\}$. It occurs in the expression for the excitation energy of the $\frac{3}{2}^+$ state in ^{41}Ar relative to the $\frac{7}{2}^-$ ground state whose value is known experimentally to be 1.035 MeV. The expression for this quantity is

$$E(\tfrac{3}{2}^+) - E(\tfrac{7}{2}^-) = 1.035 \text{ MeV}$$
$$= W(\nu f^4)_{02} + W[\pi d^{-2} \times \nu d^{-1}]_{3/2\,1/2} - W(\nu f^3)_{7/2\,3/2} - W(\pi d^{-2})_{01} + \{\epsilon_{f\nu} + {\epsilon_{d\nu}}^{-1} + 6a - \tfrac{1}{2}b\}.$$

Solving this equation gives

$$\{\epsilon_{f\nu} + {\epsilon_{d\nu}}^{-1} + 6a - \tfrac{1}{2}b\} = 7.602 \text{ MeV},$$

which in turn leads to a prediction of 2.225 MeV for the excitation energy of the core-excited 0^+ state in ^{40}Ar. This is in excellent agreement with its experimentally observed value of 2.12 MeV.

Combining the data on the $\frac{3}{2}^+$ hole states in ^{41}Ar and ^{39}Ar leads to the prediction that the excitation energy of the $[(d_{3/2})_{0,0}{}^{-4} \times (f_{7/2})_{0,3}{}^6]_{0,3}$ configuration in $^{42}_{18}Ar_{24}$ should be 1.84 MeV. At present there is no evidence for this excited 0^+ level from either the Lockheed[5] or Los Alamos[4] ^{40}Ar$(t,p)^{42}$Ar data. The Los Alamos data limit the forward-angle cross section to $\lesssim 3\%$ of the ground-state cross section for any new level between 1.207 and 2.41 MeV in ^{42}Ar.[14] On the other hand, the 0^+ state at 2.12 MeV in ^{40}Ar has a (t,p) strength $\lesssim 2\%$ of the ground-state cross section,[4] so the existence of the core-excited 0^+ state in ^{42}Ar has not been conclusively ruled out. Obviously the assumed configuration of this state would make it hard to populate in the (t,p) reaction, but it should show up strongly in the reaction $^{46}_{20}Ca_{26}(d, {}^6\text{Li})^{42}_{18}Ar_{24}$.

The position of the 2^+ core-excited states in ^{40}Ar and ^{42}Ar cannot be estimated so easily. However, by analogy with ^{42}Ca one might expect the 2.52-MeV level in ^{40}Ar to be a core-excited 2^+ state. We shall later show that the observed properties of this state support this assumption. In ^{42}Ar we might expect a core-excited 2^+ level at around 2.5 MeV. Table I summarizes some simple predictions for core-excited states in the argon isotopes.

III. MODELS

In the simplest model of the argon nuclei under consideration, one assumes that ^{40}Ca is a doubly-

TABLE I. Core-excited states in the argon isotopes: known for odd-A isotopes; predicted for even-A.

Nucleus	Spin J	Assumed configuration	Excitation energy (MeV) Predicted	Experimental
$^{37}_{18}Ar_{19}$	$\frac{7}{2}^-$	$[^{36}Ar \times f_{7/2\,1/2}]_{7/2\,1/2}$	···	1.611
$^{39}_{18}Ar_{21}$	$\frac{3}{2}^+$	$[^{37}Ar \times f_{01}^2]_{3/2\,3/2}$	···	1.517
$^{41}_{18}Ar_{23}$	$\frac{3}{2}^+$	$[^{37}Ar \times f_{02}^4]_{3/2\,5/2}$	···	1.035
$^{38}_{18}Ar_{20}$	0^+	$[^{36}Ar \times f_{01}^2]_{01}$	3.13	3.38
$^{40}_{18}Ar_{22}$	0^+	$[^{36}Ar \times f_{02}^4]_{02}$	2.23	2.12
$^{42}_{18}Ar_{24}$	0^+	$[^{36}Ar \times f_{03}^6]_{03}$	1.84	···

closed-shell nucleus, that the proton holes are restricted to the $d_{3/2}$ single-particle orbit, and that the neutrons populate the $f_{7/2}$ level. The single-particle energies and the matrix elements for the n-n and p-p residual interactions can be obtained from the binding-energy tables[13] and the spectra[15] of $^{38}_{18}Ar_{20}$ and $^{42}_{20}Ca_{22}$. These matrix elements are listed in column 3 of Table II. The hole-particle n-p interaction is taken directly from the $^{40}_{19}K_{21}$ data and is listed in Table III, column 3. With this model we cannot account for the large

TABLE II. The $T=1$ matrix elements $\langle (j_1 j_2)_J | V | (j_3 j_4)_J \rangle$ of the residual two-body interaction in the $(\nu f_{7/2})$ and $(\nu f_{7/2}, \nu p_{3/2})$ models. The upper portion of the table refers to the n-n interaction and neutron single-particle energies, the lower portion to the p-p interaction and the $d_{3/2}$ proton single-hole energy.

Configuration	J	Two-body matrix element (MeV) $(\nu f_{7/2})$	$(\nu f_{7/2}, \nu p_{3/2})$
$\frac{7}{2}\frac{7}{2}\frac{7}{2}\frac{7}{2}$	0	−3.109	−2.551
	2	−1.585	−0.753
	4	−0.358	0.015
	6	0.081	0.106
$\frac{7}{2}\frac{7}{2}\frac{7}{2}\frac{3}{2}$	2	···	−0.453
	4	···	−0.628
$\frac{7}{2}\frac{7}{2}\frac{3}{2}\frac{3}{2}$	0	···	−1.463
	2	···	−1.657
$\frac{7}{2}\frac{3}{2}\frac{7}{2}\frac{3}{2}$	2	···	−0.677
	3	···	−1.740
	4	···	1.324
	5	···	0.597
$\frac{7}{2}\frac{3}{2}\frac{3}{2}\frac{3}{2}$	2	···	0.252
$\frac{3}{2}\frac{3}{2}\frac{3}{2}\frac{3}{2}$	0	···	−1.568
	2	···	−0.537
s.p. $f_{7/2}$ energy		−8.364	−8.399
s.p. $p_{3/2}$ energy		···	−6.358
$\frac{3}{2}\frac{3}{2}\frac{3}{2}\frac{3}{2}$	0	−1.949	−1.796
	2	+0.218	+0.420
$d_{3/2}$ hole energy		+8.329	+8.258

$l_n=1$ spectroscopic strength observed at low excitation energies in $^{38}Ar(d,p)$ and $^{40}Ar(d,p)$ studies.[15] In addition, fewer states below 3 MeV are predicted than are observed experimentally.

The second model we have used to interpret the data is the one in which ^{40}Ca is again assumed to be an inert core and the proton holes are restricted to the $d_{3/2}$ single-particle orbit; but here we allow neutrons to occupy both the $f_{7/2}$ and $p_{3/2}$ orbits. With this model we can account for the existence of low-lying $\frac{3}{2}^-$ states with large $l_n=1$ spectroscopic factors. Of course, this model is unable to predict states corresponding to core excitation of a $d_{3/2}$ nucleon to the (fp) shell. In addition, some states[15] above about 3.5 MeV in ^{38}Ar (e.g., the 2^+ at 3.936 MeV) almost certainly correspond to excitation from the $d_{5/2}$ or $s_{1/2}$ to the $d_{3/2}$ level. Thus states having these spins and about these excitation energies might be expected to be missing in ^{40}Ar and ^{42}Ar.

In our calculations the matrix elements of the residual two-body interaction were taken as parameters in a least-squares fit to the experimental data. The p-p interaction and proton-hole energy in the last three lines of column 4, Table II, were determined by making a least-squares fit to the excitation energy of the first 2^+ state in ^{38}Ar and to the difference between the binding energies of ^{36}S, ^{37}Cl, ^{38}Ar, and ^{39}K relative to ^{40}Ca.

The n-n interaction listed in the last column of Table II was determined by fitting the Ca binding energies listed in Table IV and the experimental levels indicated by asterisks in Figs. 1(a) and 1(b). In making this fit, the calculations of McGrory, Wildenthal, and Halbert[16] were used as a guide in choosing those states likely to arise from the $(f_{7/2}, p_{3/2})$ model space. In particular, we have assumed that the second 0^+ and 2^+ levels in ^{42}Ca, ^{44}Ca, and ^{46}Ca do not arise from our truncated space. Moreover, we assumed that these states do not have appreciable admixtures of $(f_{7/2}, p_{3/2})$ in their wave functions so that their presence does not materially affect the other 0^+ and 2^+ states in the nuclei. We fitted 48 pieces of data and the rms error in any one of the fitted levels was 128 keV. Predictions from this fit are compared with experiments in Figs. 1(a) and 1(b).

Our calculations differ from those of Federman and Talmi[17] in two respects. First, we allow all possible excitations of $f_{7/2}$ particles to the $p_{3/2}$ orbit while they restricted themselves to at most, two-particle excitations. Second, and of greater importance, is our selection of data. Appreciably more experimental results are available now than when they made their fit. We excluded the first excited 0^+ state in ^{42}Ca, ^{44}Ca, and ^{46}Ca. They assumed that in ^{44}Ca and ^{46}Ca this state existed

TABLE III. Neutron-proton particle-hole matrix elements for the indicated models. In determining the matrix elements, we assumed in Set A that the 1.4-MeV state in ^{37}S was the single-particle $p_{3/2}$ level and in Set B that the 0.7-MeV level was this state. The last column gives the matrix elements that would apply if the surface δ interaction of Eq. (2) were used. Our convention for the nuclear radial wave functions is that they are positive at the origin.

Configuration $(\pi j_1^{-1}\nu j_2 : \pi j_1^{-1}\nu j_3)$	J	Two-body matrix element (MeV) $(\pi d_{3/2})^{-1}(\nu f_{7/2})$ model	$(\pi d_{3/2})^{-1}$ Set A	$(\nu f_{7/2}, \nu p_{3/2})$ Set B	Surface δ
$\frac{3}{2}^+\frac{7}{2}^- : \frac{3}{2}^+\frac{7}{2}^-$	2	1.364	1.277	1.332	1.371
	3	0.594	0.690	0.761	0.686
	4	0.564	0.576	0.552	0.305
	5	1.454	1.361	1.348	1.309
$\frac{3}{2}^+\frac{7}{2}^- : \frac{3}{2}^+\frac{3}{2}^-$	2		0.188	0.057	0.513
	3		0.346	0.288	0.876
$\frac{3}{2}^+\frac{3}{2}^- : \frac{3}{2}^+\frac{3}{2}^-$	0		1.212	1.150	1.600
	1		1.015	1.000	1.013
	2		0.512	0.561	0.320
	3		0.838	0.473	1.166

within the $(f_{7/2}, p_{3/2})$ model space. The importance of including the $\frac{1}{2}^-$ states of ^{43}Ca and ^{45}Ca in the fit has been pointed out by McGrory and Wildenthal[10] – in fact, the Federman-Talmi fit places the lowest $\frac{1}{2}^-$ states in these two nuclei at 5.68 and 0.89 MeV, as compared with the experimental values of 2.61 and 2.256 MeV. The exclusion of the 0^+ states and the inclusion of the $\frac{1}{2}^-$ levels does not greatly alter most of the two-body matrix elements. Exceptions are the diagonal $J=2$, 3, and 4 matrix elements of the $(f_{7/2}, p_{3/2})_J$ configuration.

The neutron-proton interaction was determined by fitting to the existing data on the binding energies and low-lying states of the S, Cl, Ar, and K isotopes. Data included in the fit to determine the proton-neutron particle-hole matrix elements are indicated by asterisks in Figs. 2–4. Those binding energies included are shown in Table V. The particle-hole matrix elements that emerged from the fit are listed as Set A and Set B in Table III. The position of the $p_{3/2}$ single-particle state in ^{37}S is not known experimentally. We first assumed that the 1.4-MeV excited state corresponded to this level. The matrix elements for this fit and the results of the fit are labeled as Set A in Figs. 2–4. The Set B results were obtained from the assumption that the 0.7-MeV state in ^{37}S was the $p_{3/2}$ level. Most of the fitted data are ground states and low-lying excited states, so that $(\pi d_{3/2})^{-1}$-$(\nu f_{7/2})$ interaction is much better determined than is the $(\pi d_{3/2})^{-1}$-$(\nu p_{3/2})$. The $(\pi d_{3/2})^{-1}(\nu p_{3/2})$ quartet in ^{38}Cl and ^{40}K has been tentatively identified.[18] However, the $l_n=1$ stripping strength in these nuclei is badly fractionated[15] and the $M1$ decay properties of the levels[19] indicate that they are far from pure states. Since there are very few ways of making a 0^- state, only this level of the $(\pi d_{3/2})^{-1}(\nu p_{3/2})$ quartets was included in the fit. Unfortunately, if the $J=1$ particle-hole matrix element was not constrained, it took on a negative value and consequently led to a very low-lying 1^- state in ^{40}K. To remedy this defect, our fit included a 1^- state at 2.5 MeV in ^{40}K. This level was sufficient to constrain the diagonal $[(\pi d_{3/2})^{-1}(\nu p_{3/2})]_{J=1}$ matrix element to a reasonable value. In actual fact, ^{40}K has an $l_n=1$ 1^- state at 2.104 MeV; but as stated before, the $l_n=1$ stripping strength is badly fractionated and consequently the "pure" state would be expected to lie above this level. Figure 2 compares the experimental spectra for ^{38}Cl and ^{40}K with our predictions for the $(\pi d_{3/2})^{-1}(\nu p_{3/2})$ and $(\pi d_{3/2})^{-1}(\nu f_{7/2})$

TABLE IV. Ground-state binding energies of the calcium isotopes fitted in determining the $(\nu f_{7/2}, \nu p_{3/2})$ $T=1$ two-body matrix elements.

Nucleus	J^π	Binding energy (MeV) Experiment	Theory
^{41}Ca	$\frac{7}{2}^-$	−8.364	−8.399
^{42}Ca	0^+	−19.837	−19.741
^{43}Ca	$\frac{7}{2}^-$	−27.769	−27.809
^{44}Ca	0^+	−38.906	−38.832
^{45}Ca	$\frac{7}{2}^-$	−46.320	−46.422
^{46}Ca	0^+	−56.724	−56.818
^{47}Ca	$\frac{7}{2}^-$	−64.000	−64.019
^{48}Ca	0^+	−73.951	−73.861
^{49}Ca	$\frac{3}{2}^-$	−79.093	−78.913
^{50}Ca	0^+	−85.450	−85.597

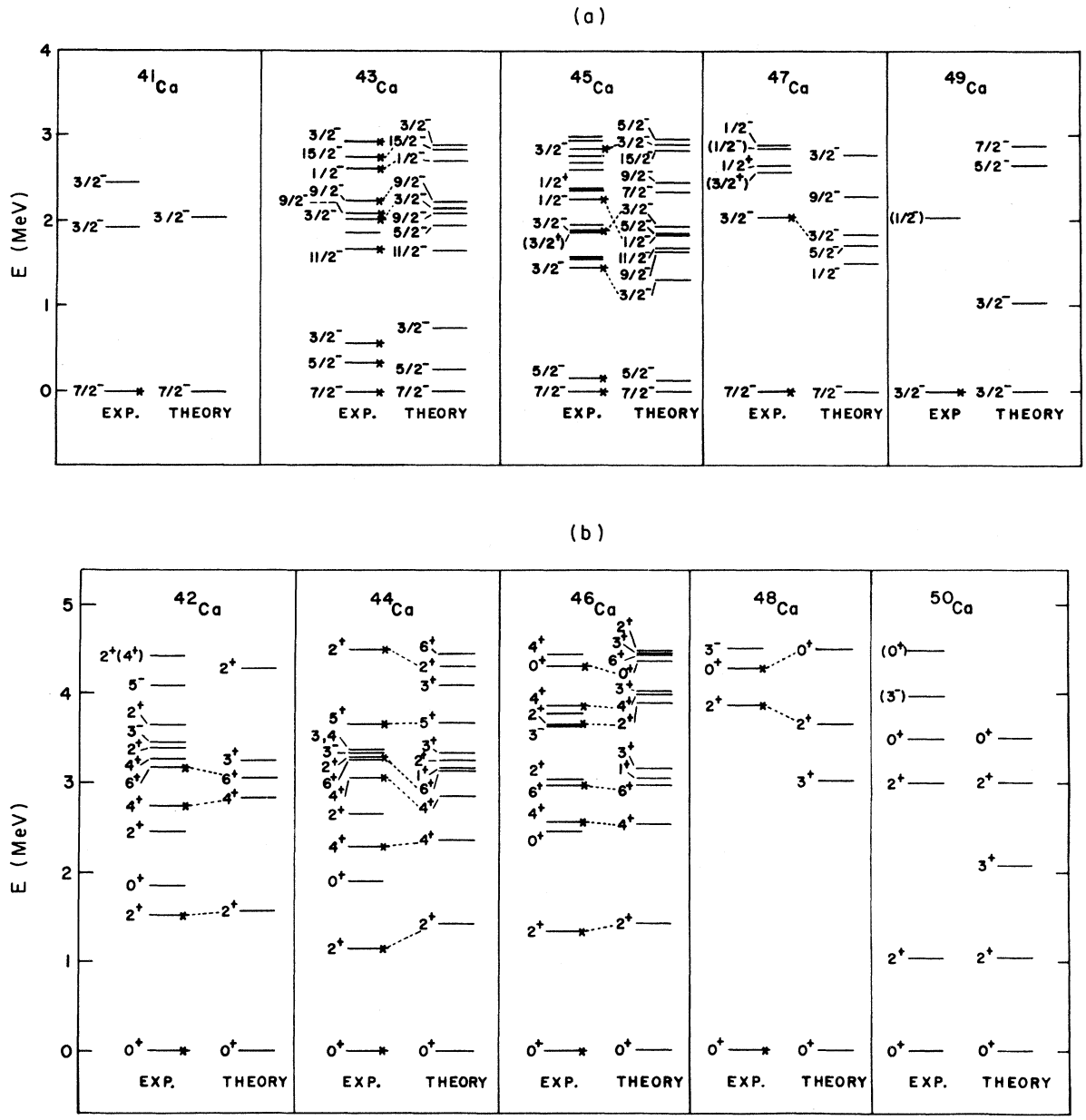

FIG. 1. Experimental and theoretical energy levels for the calcium isotopes. (a) Odd-A isotopes. Except for the $\frac{3}{2}^-$ state in ^{41}Ca (which was fitted to 2.1 MeV), all experimental levels included in the determination of the $T=1$ neutron-neutron matrix elements are indicated by an asterisk. Fitted levels are connected to the resulting theoretical levels by dotted lines. Below 3.0 MeV, all states are shown. The experimental data for ^{41}Ca were taken from F. Stechner-Rasmussen *et al.*, Nucl. Phys. A181, 225 (1972). The energy and spin for the $\frac{3}{2}^-$(2.939) state in ^{43}Ca were taken from W. E. Dorenbusch *et al.*, Phys. Rev. 146, 734 (1966). Other data for ^{43}Ca were taken from H. Gruppelaar, Nucl. Phys. A179, 737 (1972). Data for ^{45,47,49}Ca were taken from Nucl. Data B4(Nos. 3–4), 237, 313, 397 (1970). (b) Even-A isotopes. The data for ^{42}Ca were taken from E. P. Lippencott *et al.*, Phys. Rev. 163, 1170 (1967). The energy for the 5^+ state in ^{44}Ca was taken from J. H. Bjerregaard *et al.*, Nucl. Phys. A103, 33 (1967), and its spin was fixed by analogy with the 5^+ in ^{52}Cr [M. S. Freedman *et al.*, Phys. Rev. 146, 791 (1966)]. Other data in ^{44}Ca were taken from D. H. White *et al.*, Phys. Rev C 5, 513 (1972) and J. H. Bjerregaard *et al.*, Phys. Rev. 155, 1229 (1967). The 2^+(3.637), 4^+(3.959), and 0^+(4.32) states in ^{46}Ca were taken from G. M. Crawley *et al.*, Bull. Am. Phys. Soc. 17, 535 (1972). Other states in ^{46}Ca and states in ^{48}Ca were taken from Nucl. Data B4(Nos. 3-4), 269, 351 (1970). Data for ^{50}Ca were taken from R. L. Auble, Nucl. Data B3(Nos. 3, 6) 3–5, 6–1 (1970).

multiplets in ^{40}K and the corresponding particle-particle multiplets in ^{38}Cl.

Some ambiguity remains in the determination of the sign of the off-diagonal n-p matrix elements for $J=2$ and 3. There is a local minimum in the least-squares fit for both positive and negative values of these particle-hole interaction energies. Indeed, the fit to the spectra was somewhat better for negative than for positive values of these elements. On the other hand, transition rates are better reproduced for positive values of these matrix elements. To discover which sign is more appropriate, we have calculated the particle-hole interaction energies of the surface δ interaction

$$V=4\pi\delta(\Omega_{12})[0.9+0.1\sigma_1\cdot\sigma_2] \quad (5)$$

and have listed them in the last column of Table III. Since the surface δ force gives a reasonable fit to the nuclei in the (ds) shell,[20] we have chosen the signs to be positive in agreement with the predictions made by use of this interaction.

We fitted the 10 two-body particle-hole matrix elements to the 28 level energies indicated by asterisks in Figs. 2–4. For Set A (which includes the $\nu p_{3/2}$ level in ^{37}S at 1.4 MeV), the rms error in any one of the fitted levels is 152 keV. For Set B (which includes the $\nu p_{3/2}$ level in ^{37}S at 0.7 MeV), the rms error is 137 keV.

A choice between Set A and Set B cannot be made by comparing spectra. Set A has a desirable feature in that it predicts the states of the upper quartets in ^{38}Cl and ^{40}K to lie above their observed positions (as seen in Fig. 2), while Set B predicts them near observed levels of the correct spin and parity. However, for most other experimental states for which configuration mixing from outside our model space is not as important, the results of Set A and Set B are comparable.

In calculating $E2$ transition rates, we have evaluated $\langle r^2\rangle$ using harmonic-oscillator wave functions with $\hbar\omega=41A^{-1/3}$. There is some ambiguity in the measured lifetime[21,22] of the first 2^+ level in ^{38}Ar, which we have used to determine the proton effective charge. We have chosen to use the results of Ref. 21 which give $\tau_m=540$ fsec

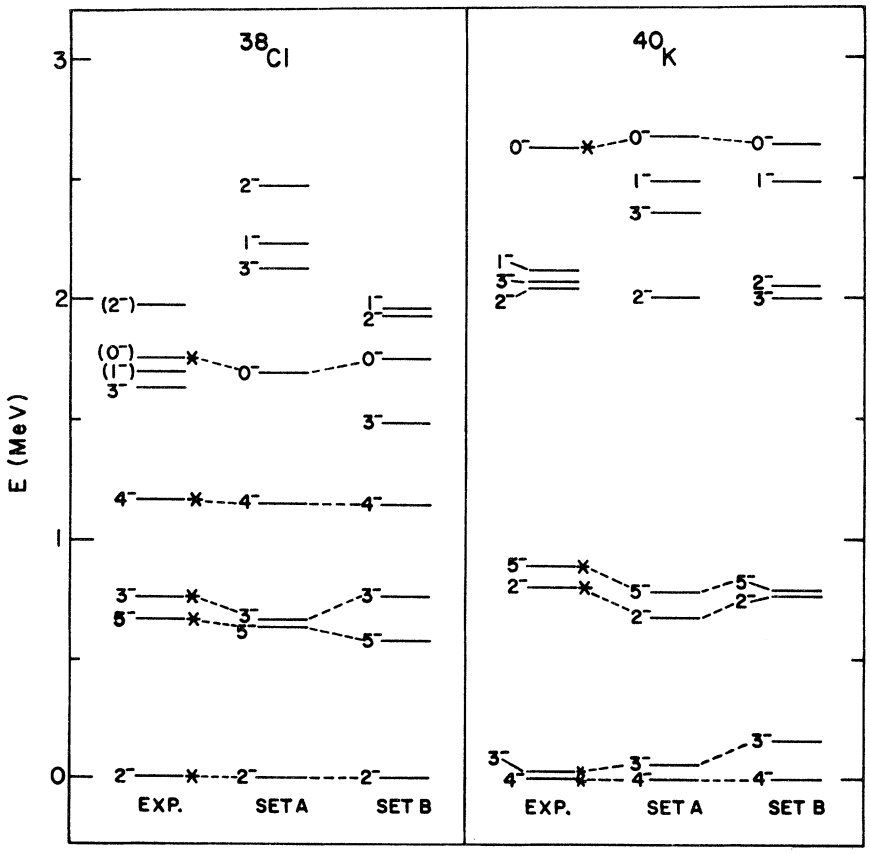

FIG. 2. Experimental and theoretical levels for ^{38}Cl and ^{40}K. The meanings of the asterisks and dotted lines are the same as in Fig. 1. The experimental data for ^{38}Cl were taken from G. A. P. Engelbertink *et al.*, Phys. Rev. C 5, 431 (1972), those for ^{40}K from R. Wechsung *et al.*, Nucl. Phys. A170, 557 (1971).

for the lifetime of the 2.1677-MeV level. To fit this result we take $e_p = 1.87e$. The neutron effective charge can be deduced[23] from the value of $B(E2; 2^+ \rightarrow 0^+)$ for ^{42}Ca. For the pure $f_{7/2}$ model, $e_n = 2.11e$; and for the $(f_{7/2}, p_{3/2})$ model, $e_n = 1.94e$. This latter value depends on the assumption that the effective neutron charge is the same for an $f_{7/2} \rightarrow f_{7/2}$, a $p_{3/2} \rightarrow p_{3/2}$, and a $p_{3/2} \rightarrow f_{7/2}$ transition. Actually the $\frac{3}{2}^- \rightarrow \frac{7}{2}^-$ lifetime (Ref. 15) in ^{41}Ca requires that $e_n(p_{3/2} \rightarrow f_{7/2}) = 1.344e$. We have therefore made calculations within the $(f_{7/2}, p_{3/2})$model, using the state-independent value $e_n = 1.94e$ and the state-dependent values $e_n(p_{3/2} \rightarrow f_{7/2}) = 1.344e$ and $e_n(f_{7/2} \rightarrow f_{7/2}) = e_n(p_{3/2} \rightarrow p_{3/2}) = 1.95e$.

For $M1$ transitions there are also several possible values for each of the parameters that enter into the effective operators. We have made calculations in which the magnetic moment of the proton and neutron have their free values $\mu_p = 2.79\mu_N$ and $\mu_n = -1.91\mu_N$. We have also examined the case in which $\mu_n(f_{7/2}) = -1.595\mu_N$ (the value needed to fit the ^{41}Ca ground-state magnetic moment) and $\mu_n(p_{3/2}) = -1.91\mu_N$. For the proton, the values $\mu_p = 1.86\mu_N$ and $\mu_p = 2.348\mu_N$ (the values needed to fit the ground-state magnetic moments of ^{37}Cl and ^{39}K, respectively, have been considered.

IV. RESULTS

A. $^{39}_{18}Ar_{21}$

The theoretical and experimental level sequences for this nucleus are compared in Fig. 3. The main shortcoming of the $(\pi d_{3/2})^{-2}(\nu f_{7/2})$ model is that it provides only one $\frac{3}{2}^-$ state. To remedy this defect and to obtain states that exhibit $l_n = 1$ stripping, it is necessary to include the neutron $p_{3/2}$ orbital. With this extended model, the two observed $\frac{3}{2}^-$ states at 1.267 and 2.63 MeV can be reproduced reasonably well with either Set A or Set B matrix elements (as seen in Fig. 3). However, even with the extended $(\pi d_{3/2})^{-2}(\nu f_{7/2}, \nu p_{3/2})$ model space we do not get the observed density of presumed negative-parity states that lie below 3 MeV.

Neutron stripping on ^{38}Ar indicates that the 2.093-MeV level in ^{39}Ar has a weak $l_n = 3$ shape.[24] For this reason the level had previously been assigned a $\frac{7}{2}^-$ spin. Recently, however, Bass and Saleh-Bass[25] measured the branching ratio for the

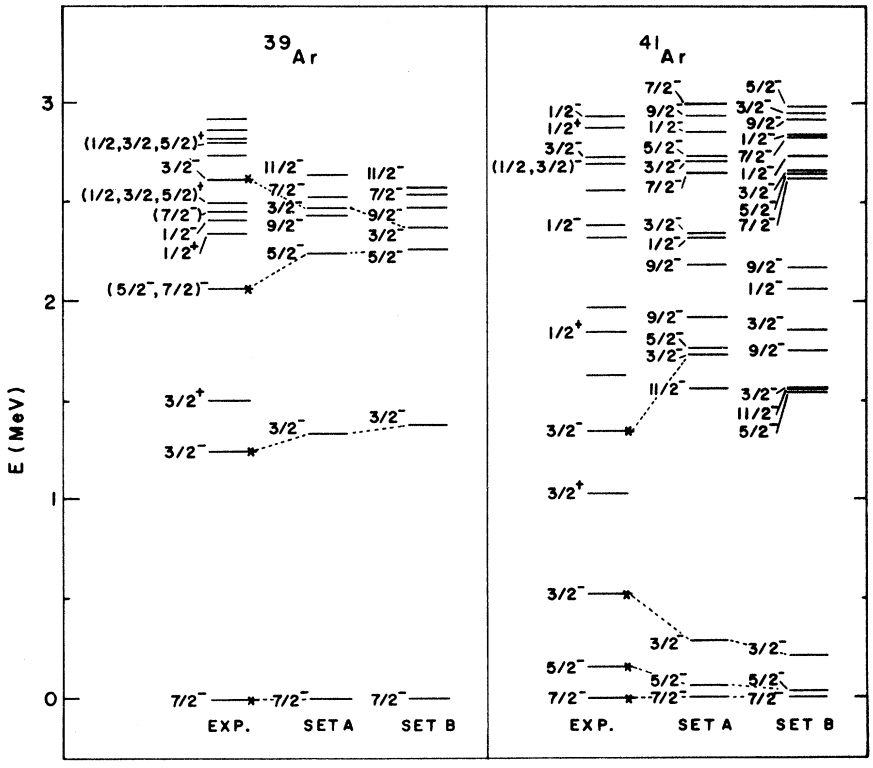

FIG. 3. Experimental and theoretical levels for ^{39}Ar and ^{41}Ar. The meanings of the asterisks and dotted lines are the same as in Fig. 1. All states up to 3.0 MeV are shown. The data for ^{39}Ar were taken from Ref. 28 and from S. Sen *et al.*, Phys. Rev. C 5, 1278 (1972). Data for ^{41}Ar were taken from Refs. 31 and 32, and from F. Stecher-Rasmussen *et al.*, Nucl. Phys. A181, 225 (1972).

decay from the 2.63-MeV second $\frac{3}{2}^-$ state to this level and to the ground state. On the assumption that the 2.093 level has spin $\frac{7}{2}^-$, this branching ratio would be the ratio of the fifth powers of the energies if the single-particle model were used. That is,

$$R_{s.p.} = (2.63/0.537)^5 = 2818 .$$

Experimentally, this ratio is 1.9 ± 1.2. Thus it seems unlikely that the 2.093-MeV state is $\frac{7}{2}^-$. As seen in Fig. 3, a $\frac{5}{2}^-$ state is predicted in both our calculations at approximately this excitation. Moreover, since a 1% $f_{5/2}$ admixture into the ground state of ^{38}Ar could explain the stripping data (Ref. 24), we have made a $\frac{5}{2}^-$ assignment for this state in all our calculations.

At present there are no measured lifetimes for the negative-parity states in ^{39}Ar. Our predicted lifetimes are listed in Table VI. These results were obtained with the effective charges $e_p = 1.87e$ and $e_n = 1.94e$ for $E2$ rates and with the free values for the magnetic moments of the proton and neutron. With the exception of the $E2$ lifetimes of the $\frac{3}{2}^-$ states (which we shall discuss below) very

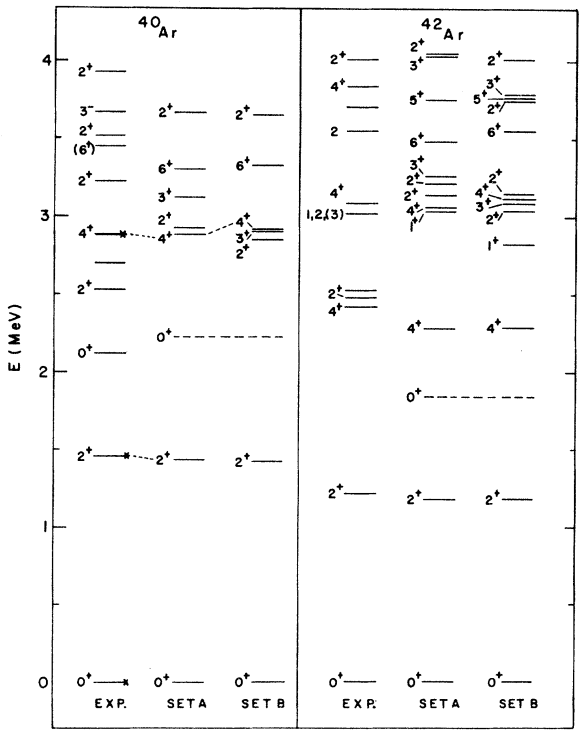

FIG. 4. Experimental and theoretical levels for ^{40}Ar and ^{42}Ar. The meanings of the asterisks and dotted lines are the same as in Fig. 1. All states up to 4.1 MeV are shown. The data for ^{40}Ar were taken from Refs. 1–4, those for ^{42}Ar from Refs. 4 and 5. The predicted core-excited 0^+ level is shown with a dotted line.

TABLE V. Ground-state binding energies fitted in determining the proton-neutron particle-hole matrix elements.

Nucleus	J^π	Binding energies (MeV) Exp.	Set A	Set B
$^{40}_{19}K_{21}$	4^-	0.529	0.435	0.411
$^{41}_{19}K_{22}$	$\frac{3}{2}^+$	−9.568	−9.830	−9.816
$^{42}_{19}K_{23}$	2^-	−17.102	−17.397	−17.331
$^{39}_{18}Ar_{21}$	$\frac{7}{2}^-$	8.111	8.062	8.086
$^{40}_{18}Ar_{22}$	0^+	−1.759	−1.655	−1.632
$^{41}_{18}Ar_{23}$	$\frac{7}{2}^-$	−7.858	−7.861	−7.811
$^{38}_{17}Cl_{21}$	2^-	18.841	18.763	18.803
$^{39}_{17}Cl_{22}$	$\frac{3}{2}^+$	10.767	10.690	10.672
$^{40}_{17}Cl_{23}$	2^-	4.963	4.968	4.959
$^{37}_{16}S_{21}$	$\frac{7}{2}^-$	29.023	28.858	28.910
$^{38}_{16}S_{22}$	0^+	20.995	21.306	21.213

TABLE VI. Predicted mean lifetimes τ_m for transitions in ^{39}Ar. The theoretical initial and final states are specified by their values of J^π. The experimental transition energies E_γ^{exp} used in calculating the partial lifetimes were taken from Ref. 28 and S. Sen *et al.*, Phys. Rev. C 5, 1278 (1972). The partial mean lifetimes for Set A (upper number in each case) and for Set B (lower number) are given in psec in column 4 and in Moszkowski units (theoretical lifetime relative to single-particle estimate) in column 5.

Initial state	Final state	E_γ^{exp} (MeV)	Mean lifetime (psec)	(M.u.)
$\frac{5}{2}^-_1$	$\frac{3}{2}^-_1$	0.826	2.45	48.0
			5.88	115
$\frac{5}{2}^-_1$	$\frac{7}{2}^-_1$	2.093	0.360	164
			0.349	159
$\frac{3}{2}^-_2$	$\frac{5}{2}^-_1$	0.537	2.99	24.2
			2.29	18.5
$\frac{3}{2}^-_1$	$\frac{7}{2}^-_1$	1.267	1.46	0.119
			1.48	0.121
$\frac{3}{2}^-_2$	$\frac{7}{2}^-_1$	2.63	1.88	5.95
			4.72	14.9
$\frac{7}{2}^-_2$	$\frac{5}{2}^-_1$	0.391	7.49	16.7
			7.58	16.9
$\frac{7}{2}^-_2$	$\frac{3}{2}^-_1$	1.217	346	11.6
			134	4.50
$\frac{7}{2}^-_2$	$\frac{7}{2}^-_1$	2.484	1.43	760
			1.39	738

similar values result when state-dependent charges are used. The $M1$ transition dominates in all cases where angular momentum changes by 0 or ±1.

Branching ratios for the decay of various levels (Ref. 25) are tabulated in Table VII, together with the single-particle estimate[26] and our theoretical predictions. From the first line of the table we can conclude that the branching ratio predicted by either Set A or Set B is consistent with the data. However, this agreement for the $\frac{3}{2}^-(2.63) \rightarrow \frac{7}{2}^-$(g.s.) transition may be fortuitous since there is strong destructive interference between the contributions from the proton and neutron $E2$ operators. If state-dependent effective charges are used (as suggested in the last paragraph of Sec. III), the interference becomes nearly complete for Set A matrix elements. The branching ratio becomes 4.8×10^{-3} for Set A and 2.2 for Set B matrix elements. For the second and last entries to Table VII, $M1$ transitions dominate, and agreement between experiment and theory is good.

The observed $M1$ decay properties of the 2.484-MeV $\frac{7}{2}^-$ state are seen only through branching ratios to other states. A lifetime measurement for this level would check our predicted inhibition of 5–10. On the other hand, the one place where a branching ratio from this level depends sensitively on the $E2$ component is shown in the third line of Table VII and this is badly reproduced by our theory. A possible explanation for this is as follows: The position of the $\frac{7}{2}^-$ core excited state arising from the $[^{36}\mathrm{Ar(g.s.)} \times (\nu f_{7/2})_{7/2}{}^3]$ configuration can be estimated using the techniques of Sec. II. The known positions of the $\frac{3}{2}^+$ level in ^{41}Ar and the core excited 0^+ in ^{40}Ar allow us to predict that this core-excited state in ^{39}Ar lies at 2.6 MeV. Thus the 2.484 MeV $\frac{7}{2}^-$ level will probably have a substantial component in its wave function involving core excitation and this is likely to have an appreciable effect on the already small $E2$ matrix element. With the exception of this one branching ratio, the other γ-decay properties of the low-lying state of ^{39}Ar are reasonably well reproduced by our calculation.

In an earlier calculation[27] the $\frac{3}{2}^+$ hole state corresponding to $[^{37}\mathrm{Cl} \times (f_{7/2})_{01}{}^2]_{3/2,\,3/2}$ was predicted at about 2.3-MeV excitation energy. Engelbertink, Warburton, and Olness[28] have argued that this configuration could be dominant in the 2.503-MeV level. The state observed at 2.829 MeV is a candidate for this level, and it would be important to see if this state is populated strongly in the $^{37}\mathrm{Cl}(^3\mathrm{He}, p)^{39}\mathrm{Ar}$ reaction.

Finally, the $l_n = 3$ spectroscopic factor for neutron stripping to the ^{39}Ar ground state is anomalously small (Ref. 24). Experimentally $(2J+1)S = 4.68$; that is, in the ground-state wave function of ^{39}Ar, there is only a 58.5% probability that we will find $[^{38}\mathrm{Ar}(0^+) \times \nu f_{7/2}]$. We predict about 7.3 for this quantity with either Set A or Set B wave functions. For the $\frac{7}{2}^-$ level at 2.484 MeV, the measured value is $(2J+1)S_{\mathrm{expt}} = 0.67$ and we predict 0.57 for Set A and 0.64 for Set B. For stripping to the $\frac{3}{2}^-$ states at 1.267 and 2.63 MeV, Fitz, Jahr, and Santo[24] give $(2J+1)S_{\mathrm{expt}} = 2.09$ and 0.70, respectively. For Set A parameters our predictions are 2.59 and 1.27, whereas for Set B we obtain 3.41 and 0.56. These $l_n = 1$ stripping results sup-

TABLE VII. Branching ratios for transitions in ^{39}Ar. The experimental numbers are taken from the work of Bass and Saleh-Bass (Ref. 25). The single-particle estimates are Moszkowski values (Ref. 26). The $E2$ estimates were obtained with $e_p = 1.84e$ and $e_n = 1.94e$. The $M1$ transitions were calculated with $\mu_p = 2.79\mu_N$ and $\mu_n = -1.91\mu_N$ for the magnetic moments of the proton and neutron, respectively.

Initial state		Final state		Branching ratio		
Energy (MeV)	Spin J^π	Energy (MeV)	Spin J^π	Expt.	Single particle	Theoretical Set A/Set B
2.63	$\frac{3}{2}^-$	0	$\frac{7}{2}^-$	1.9±1.2	0.4	1.6
		2.093	$\frac{5}{2}^-$			0.5
2.093	$\frac{5}{2}^-$	0	$\frac{7}{2}^-$	8.2±2.8	23.3	6.8
		1.267	$\frac{3}{2}^-$			16.8
2.484	$\frac{7}{2}^-$	2.093	$\frac{5}{2}^-$	2.1±1.7	66.4	46.2
		1.267	$\frac{3}{2}^-$			17.7
2.484	$\frac{7}{2}^-$	0	$\frac{7}{2}^-$	3.8±2.2	238.6	5.2
		2.093	$\frac{5}{2}^-$			5.5

port the contention that the 1.4-MeV state in ^{37}S is the $\frac{3}{2}^-$ single-particle level.

B. $^{40}_{18}Ar_{22}$

The theoretical and experimental energy levels of ^{40}Ar are compared in Fig. 4. In our calculated level scheme we predict a 6^+ level at ~3.4-MeV excitation energy. Recently, the Los Alamos group[4] has seen a state at 3.46 MeV that seems to exhibit an $L=6$ shape in the (t,p) reaction. With the extended $(\nu f_{7/2}, \nu p_{3/2})$ model, we predict a 3^+ level near the 4^+ state at ~2.9 MeV. In a study of the $^{41}_{19}K_{22}(d,{}^3He)^{40}_{18}Ar_{22}$ reaction, Yntema (Ref. 3) observes the 4^+ level very weakly; on the basis of our extended model, this level should not be populated. He sees evidence for a weak $l_p=2$ transition to a state at 2.701 MeV and finds its spectroscopic factor to be only a few percent of that of the transition to the ground state. With Set A parameters, we predict that the spectroscopic factor for the transition to our model 3^+ state should be 2.4% of that for the ground-state transition. For Set B, it should be 1.4%. Thus the predicted 3^+ state has the characteristics of the observed 2.701-MeV level.

Experimentally the $E2$ transition between the ground state and the 2^+ level at 1.461 MeV is enhanced by about a factor of 10. The lifetime[15] of this state is $\tau_m = 1.2 \pm 0.3$ psec. All the models of ^{40}Ar we have used predict the correct value of τ_m. For example, the $f_{7/2}$ model, Set A, and Set B give $\tau_m = 0.92$, 0.88, and 0.90 psec, respectively. The spectroscopic factor for proton pickup to this level is predicted to be about 1.4 times that to the ground state with either set of matrix elements. Yntema finds this transition to be about $1\frac{1}{2}$ times as strong as the transition to the ground state. Thus the properties of the first excited state are well reproduced by our model.

The second 2^+ state at 2.524 MeV is observed weakly (~15% of the ground-state strength) in Yntema's pickup experiment. In our model space, the second 2^+ level is predicted to have a large spectroscopic factor: 2.83 (Set A) or 2.99 (Set B) times the ground-state value. Thus, as has already been suggested (Refs. 1 and 2), this level probably is analogous to the second 2^+ level in ^{42}Ca and therefore its wave functions has a substantial component corresponding to excitation from the ds shell to the fp shell.

On the other hand, the 2^+ level at 3.207 MeV in ^{40}Ar does have the characteristics of our second model-space 2^+ state. Its spectroscopic factor (Ref. 3) is 3.5–4 times the ground-state factor. The experimental branching ratio (Ref. 1) for the decay from this state to the 1.46-MeV 2^+ and to the ground state is

$$R = [2^+(3.207) \to 2^+(1.461)] / [2^+(3.207) \to 0^+(\text{g.s.})] = 7^{+5.7}_{-2.4}.$$

Values within the experimental error are predicted by both Set A and Set B matrix elements and with both state-dependent and state-independent effective charges.

The 2^+ state at 3.507 MeV exhibits a substantial amount of $l_p=0$ pickup in the ^{41}K$(d,{}^3$He$)^{40}$Ar experiment (Ref. 3). Consequently, its wave function must have a sizable component involving excitation from the $2s_{1/2}$ level to the $1d_{3/2}$ orbit. Such a state near this energy may be predicted from the presence of a 2^+ core-excited state[15] at 3.9 MeV in ^{38}Ar. Thus we have correlated our third model-space 2^+ state not with this level but with the 3.926-MeV state, which was observed with $L=2$ in the Los Alamos (t,p) work (Ref. 4). The predicted $M1$ decay from this state to the 1.461-MeV level is inhibited by a factor of several thousand; hence, this transition should be dominantly $E2$.

The first excited 0^+ level has already been shown to arise from excitation from the (ds) shell to the (fp) shell. The second and fourth 2^+ states also seem to involve substantial amounts of core excitation. However, the properties of the remaining levels below 4 MeV seem rather well accounted for by our $(\pi d_{3/2})^{-2}(\nu f_{7/2}, \nu p_{3/2})^2$ model.

C. $^{41}_{18}Ar_{23}$

Only the first four negative-parity states were included in the fit to the ^{41}Ar data because substantial $l_n=1$ strength to $\frac{1}{2}^-$ states is found at excitations above 2 MeV. Since the $p_{1/2}$ orbit is not considered in our calculations, it would be incorrect to distort our interaction to fit these states, which have an appreciable component lying outside our model space.

Two $M1$ lifetimes and one $E2$ lifetime have been measured in this nucleus.[29] Let us first consider the 165-keV $M1$ transition from the $\frac{5}{2}^-$ level to the ground state. The experimental mean life for this transition is 0.59 nsec, which represents an inhibition of about a factor of 140 from the Moszkowski estimate (Ref. 26). The $(\pi d_{3/2})^{-2}(\nu f_{7/2})^3$ model predicts the transition to be severely inhibited relative to the single-particle estimate – that is, the wave functions of the two states involved in the transition are almost purely $(\pi d_{3/2})_0^2(\nu f_{7/2})_1^3$ and between states of this configuration the $M1$ operator vanishes.[30] On the other hand, either Set A or Set B matrix elements give more reasonable values for this lifetime. For example, with the free values of μ_p and μ_n, Set A

leads to the prediction that $\tau_m = 3.4$ nsec and Set B to $\tau_m = 2.7$ nsec.

The second $M1$ lifetime that has been measured[29] is the 353-keV transition between the first $\frac{3}{2}^-$ and the first $\frac{5}{2}^-$ states. This transition, which is inhibited by a factor of about 5000, has a measured mean life of 2.23 nsec. Even the $(\pi d_{3/2})^{-2}(\nu f_{7/2})^3$ model gives too big a matrix element for this transition [$\tau_m(f_{7/2}) = 0.5$ nsec]. The extended model leads to a larger transition probability and hence an even shorter lifetime. Again, using the free values of μ_p and μ_n, we arrive at the prediction that $\tau_m = 0.14$ nsec (Set A) and $\tau_m = 0.08$ nsec (Set B). Even if the $M1$ matrix element is set equal to zero, the predicted $E2$ mixture alone leads to too short a lifetime for this transition; i.e., for either set of matrix elements, the $E2$ lifetime for decay to the $\frac{5}{2}^-$ level is $\tau_m \cong 0.5$ nsec, which represents $\cong$15-fold enhancement over the Moszkowski estimate.

The 518-keV decay from the $\frac{3}{2}^-$ state to the $\frac{7}{2}^-$ ground state has a lifetime that has also been measured by Fossan and Poletti.[29] From their data one obtains $\tau_m = 0.63$ nsec for this transition. From our models we obtain the substantially shorter lifetimes $\tau_m = 0.184$, 0.1020, and 0.1021 nsec for the $f_{7/2}$ model, Set A, and Set B, respectively.

Finally, the branching ratio for decay of the 1.354-MeV $\frac{3}{2}^-$ state has been studied by the Götenberg group. In their first study[31] they found that this state decayed 12% of the time to the 518-keV $\frac{3}{2}^-$ level, 85% of the time to the 167-keV $\frac{5}{2}^-$ state, and 3% of the time to the ground state. In a later study[32] these numbers were reported to be 18, 78, and 4%, respectively. In any case, the dominant decay mode was to the 165-keV $\frac{5}{2}^-$ level. Aside from the weak branch to the ground state, this is precisely the single-particle prediction. In fact, if each of the $M1$'s were inhibited by a factor of about 30, the Moszkowski estimate would be correct even for the branch to the ground state. On the other hand, both Set A and Set B matrix elements give a much more marked inhibition in the $\frac{3}{2}^- \rightarrow \frac{5}{2}^-$ transition than in the $\frac{3}{2}^- \rightarrow \frac{3}{2}^-$ (a factor of about 1000 in the former transition and about 25 in the latter), so our model gives almost equally intense branches to the 518- and 165-keV levels.

In summary, our extended $(\pi d_{3/2})^{-2}(\nu f_{7/2}, \nu p_{3/2})^3$ model reproduces the ^{41}Ar level scheme below 2 MeV reasonably well and, in agreement with observation, it predicts that all $M1$ transitions should be severely inhibited. Because of this very severe inhibition, all $M1$ matrix elements are subject to large changes due to small amounts of $\pi d_{5/2}{}^{-1}$, $\nu f_{5/2}$, or $\nu p_{1/2}$ configuration mixing. Hence, agreement with experiment would be only coincidental. The $E2$ properties of the 518-keV state are badly predicted by the model – the $E2$ transitions from this level are considerably less enhanced than predicted. Experimentally, the $\frac{3}{2}^-(0.518) \rightarrow \frac{7}{2}^-$(g.s.) transition is enhanced by a factor of 1.6 relative to the Moszkowski estimate, but its enhancement is less than that of the analogous 594-keV transition in ^{43}Ca. Using the ^{43}Ca branching ratios quoted by Fossan and Poletti[30] and the recent results of Bini *et al.*,[33] one obtains an experimental lifetime of 0.147 nsec for this transition. This represents an enhancement of 3.2 relative to the Moszkowski estimate.

D. $^{42}_{18}Ar_{24}$

None of the data on ^{42}Ar were included in the fit. In Fig. 4 our theoretical predictions are compared with the recent experimental data. The ground-state binding energy is well reproduced by either Set A or Set B matrix elements (as seen in Table V), as is the position of the first excited 2^+ state. Three $L = 4$ transitions to states below 4 MeV are observed in the (t,p) reaction.[4] In any of our models, only two such states are predicted. The energies of these two predicted states agree quite well with the two lowest observed 4^+ levels. The $(f_{7/2})^4$ configuration has two states with $J = 4$, the lower of the two having seniority four.[34] Thus our lowest predicted 4^+ state in ^{42}Ar has a wave function which is predominantly $(\pi d_{3/2})_0^2(\nu f_{7/2})_{J=4,\,v=4}^4$. The second predicted 4^+ level is again dominated by neutron excitation, but in this case the seniority of the state is $v = 2$. If the (t,p) process is a direct reaction, then the maximum change in seniority allowed by the precess is $\Delta v = \pm 2$. Consequently, if one assumes that ^{40}Ar has a seniority-zero ground state, the seniority-four part of the 2.414-MeV state should not be populated in the reaction. Experimentally,[4] the 3.092-MeV level is $2\frac{1}{2}$ times more strongly excited than the 2.414-MeV state, in agreement with the theoretical expectations.

The predicted $E2$ lifetime of the first excited state is $\tau_m = 1.89$, 1.89, and 1.86 psec for the $f_{7/2}$ model, Set A, and Set B, respectively. In all cases this represents a substantial enhancement over the single-particle estimate.

From Fig. 4 it can be seen that the 0^+(g.s.), $2^+(1.377)$, $4^+(2.414)$, and $4^+(3.092)$ experimental states correlate well with our model states. We shall now discuss the properties of the remaining observed and predicted states and make some tentative suggestions about possible correspondences between them.

The correlation work[5] established that the 2.485-MeV state has spin 2^+. We predict a pair of 2^+ levels at around 3.2 MeV. However, in analogy

with ^{40}Ar, ^{42}Ca, and ^{44}Ca, in which a core-excited 2^+ state is seen at 2.524, 2.423, and 2.657 MeV, respectively, we would expect this level to have a wave function that involves substantial excitation from the (ds) shell to the (fp) shell.

The 2.510-MeV level is seen weakly[4] in the (t,p) reaction. The γ decay of this state is predominantly ($\geq$90%) to the first excited 2^+ level, with only a small or vanishing branch ($\leq$10%) to the ground state. It is possible that this state is our predicted core-excited 0^+ level, although the energy is considerably (~700 keV) higher than we would have anticipated. If the spin of the state were 1^+, the single-particle estimate would favor the ground-state branch by a factor of about 7. Both Set A and Set B matrix elements predict a 1^+ state at about 3 MeV. In addition, both models predict that the $1_1^+ \rightarrow 0_1^+$ transition should be inhibited by about a factor of 35 relative to the $1_1^+ \rightarrow 2_1^+$ decay. If the 2.510-MeV state is the second model 2^+ level (Fig. 4), then the observed branching ratio could not be explained as well. With either Set A or Set B matrix elements, this ratio is predicted to be about 2:1. A spin of 3^+ would also explain that the γ-decay data are consistent with our prediction of a 3^+ level at around 3-MeV excitation energy.

The 3.012-MeV level has the possible spin values 1, 2, or 3. Because a branch to the ground state is seen, the 3^+ assignment seems unlikely. If the spin is 1^+, our calculations would predict that the branch to the ground state should be inhibited by a factor of about 35 relative to that to the 1.207-MeV level, in agreement with experiment.

Turning now to the 3.555-MeV level, which has a spin of 2^+, we find that if one assumes that this is the third model-space 2^+ level, its predicted γ branching ratio $(2_3^+ \rightarrow 2_1^+)/(2_3^+ \rightarrow 0_1^+)$ is about 15:1 for either Set A or Set B. This is to be compared with the Lockheed result[5] of 6.2 ± 1.9.

Our preferred identifications of the energy levels in this nucleus are: 2.485 MeV, core-excited 2^+ state; 2.510 MeV, first model-space 3^+ or 1^+ state; 3.012 MeV, first model-space 1^+ or 3^+ state; and 3.555 MeV, third model-space 2^+ state. If these identifications are correct, three of the levels that Set A predicts below 4 MeV excitation have not yet been seen. These are the 2^+, 6^+, and 5^+ levels that should lie near 3, 3.5, and 4 MeV, respectively. A possible candidate for the 6^+ level might be the 3.70-MeV state, which is seen with moderate strength in the (t,p) reaction.[4] Set B matrix elements lead to a more compressed level scheme and give rise to two additional levels below 4 MeV – a fourth 2^+ state and a second 3^+. For Set A, the predicted energies of these states are only slightly above 4 MeV, at 4.055 and 4.041 MeV, respectively. Of these, the predicted 2^+ state could perhaps be identified with the 2^+ level observed at 4.006 MeV.

V. DISCUSSION

In the preceding sections we have discussed the properties of the Ar isotopes with $N \geq 21$ on the basis of several models. The first was the simple $(\pi d_{3/2})^{-2}(\nu f_{7/2})^n$ model. The matrix elements for the neutron-neutron interaction were taken from the ^{42}Ca data, those for the proton-proton interaction from the binding energies of ^{38}Ar and ^{39}K relative to ^{40}Ca along with the excitation energy of the first 2^+ state in ^{38}Ar, and those for the proton-neutron interaction from ^{40}K. The most obvious shortcomings of this model are that it does not allow for any $l_n = 1$ stripping strength and that for odd-A nuclei it misses one low-lying $\frac{3}{2}^-$ state.

To remedy these defects we included the effects of the $2p_{3/2}$ neutron orbital. In this case, the matrix elements of the neutron-neutron interaction were varied so as to give a best fit to the Ca data, the levels used in this determination being those indicated by asterisks in Fig. 1; the matrix elements for the proton-proton interaction were adjusted to fit the excitation energy of the 2^+ level in ^{38}Ar and the binding energies of the $N=20$ isotones with $16 \leq Z < 20$; and the levels marked with asterisks in Figs. 2, 3, and 4 were fitted to determine the neutron-proton interaction. Because of the paucity of data, the diagonal matrix elements of the $(\pi d_{3/2})^{-1}(\nu p_{3/2})$ interaction were not as well determined as those of the $(\pi d_{3/2})^{-1}(\nu f_{7/2})$ interaction. Further, there was an ambiguity in the sign of the off-diagonal

$$\langle (\pi d_{3/2}{}^{-1}, \nu p_{3/2})_J \,|\, V \,|\, (\pi d_{3/2}{}^{-1}, \nu f_{7/2})_J \rangle$$

matrix elements with $J=2$ and 3. The signs of both matrix elements were chosen to be positive because this sign gave a best fit to the transition-rate data and because this sign is predicted by the surface δ interaction. With this extended model space, the Ar data can be fitted reasonably well and on this basis one can predict the number of low-lying $\frac{3}{2}^-$ levels. In addition, in the even-A nuclei one predicts the existence of 1^+ and 3^+ levels at low energies (~3 MeV), a feature that the $f_{7/2}$ model did not provide. In ^{40}Ar the data on the ^{41}K$(d, {}^3\mathrm{He})^{40}$Ar reaction[3] now provide some evidence for an additional weak $l_p = 2$ state, which does not fit into the $f_{7/2}$ picture. This new state occurs at about the energy of the predicted 3^+ level. In agreement with the $f_{7/2}$ model, this extended model predicts rather severe inhibition (factors of 10 or more) of $M1$ transitions between

low-lying states. One must view our $M1$ predictions with some skepticism since small admixtures of $\pi d_{5/2}^{-1}$, $\nu f_{5/2}$, or $\nu p_{1/2}$ into the wave functions could substantially change an almost vanishing matrix element. In addition to the $M1$ problem, the model has other shortcomings. In the odd-mass Ar nuclei there is evidence for a low-lying $\frac{3}{2}^+$ state that arises from excitation from the ds shell to the fp shell. At ~2.5 MeV in ^{40}Ar, there is evidence for low-lying 0^+ and 2^+ levels that lie outside the $(\pi d_{3/2})^{-2}(\nu f_{7/2}, \nu p_{3/2})^2$ model space.

Several experiments would help to clarify the situation in these Ar nuclei.

(1) We have discussed these nuclei with the aid of two different $(\pi d_{3/2})^{-2}(\nu f_{7/2}, \nu p_{3/2})^n$ models: Set A in which we assumed that the 1.4-MeV excited state in ^{37}S was the $p_{3/2}$ single-particle orbital and Set B in which we assumed that the 0.7-MeV level was the $p_{3/2}$ state. The advantage of Set A is that it leads to a somewhat less condensed level scheme and spreads out the $l_n=1$ spectroscopic strength, while Set B gives a slightly better fit to the data. By analogy with ^{41}Ca the $p_{3/2}$ single-particle strength might be expected to be spread over several states. The ^{36}S$(d,p)^{37}$S reaction should be used to locate the centroid of the $\frac{3}{2}^-$ states in ^{37}S and test the assumptions used in this paper.

(2) Simple binding energy considerations lead to the prediction of a core-excited 0^+ state in ^{42}Ar at about 1.8-MeV excitation energy. This state should show up only weakly (if at all) in the (t,p) reaction and, indeed, it has not been seen. On the other hand, one would expect to see it strongly in an α-pickup reaction on ^{46}Ca, for example, in ^{46}Ca$(d,{}^6\mathrm{Li})^{42}$Ar. (Similar considerations lead to the prediction of an excited 0^+ state in ^{40}Ar at about 2.2 MeV, which has been observed.)

(3) At about 3-MeV excitation energy in ^{39}Ar there should be a core-excited $J=\frac{3}{2}^+$, $T=\frac{3}{2}$ state whose configuration is predominantly ^{37}Cl in its ground state plus two $f_{7/2}$ particles coupled to $J=0$. Thus it would be useful to study the ^{37}Cl-$(^3\mathrm{He},p)^{39}$Ar reaction to search for this state.

(4) In the ^{38}Ar$(t,p)^{40}$Ar reaction, an $L=6$ state has been tentatively identified at 3.46 MeV.[4] The theoretical prediction for the excitation energy of the $J=6$ state in this nucleus is 3.3 MeV. In ^{42}Ar a 6^+ state is predicted at about 3.5 MeV, and it would be surprising if the theoretical predictions were not borne out by experiment.

(5) In ^{39}Ar the 2.093-MeV state is observed via $l_n=3$ transfer.[24] We predict a $\frac{5}{2}^-$ spin assignment for this level. It would, therefore, be interesting and important to have additional information on the spin of this state.

(6) In calculating $E2$ lifetimes, we made two different assumptions. First, we assumed a state-independent effective neutron charge $e_n=1.94e$, which was the value needed to fit the $B(E2)$ in ^{42}Ca. On the other hand, the lifetime of the $\frac{3}{2}^-$ state in ^{41}Ca indicates that the effective neutron charge for a $p_{3/2}\rightarrow f_{7/2}$ transition may have the smaller value $e_n(p_{3/2}\rightarrow f_{7/2})=1.344e$. For the first 2^+ state in the even-even nuclei, there is little difference between the predicted lifetimes based on these two assumptions. For the $\frac{3}{2}^-(1.267)\rightarrow\frac{7}{2}^-$(g.s.) transition in ^{39}Ar, however, the predictions differ in that the lifetime based on a state-dependent effective charge is twice as long as that predicted on the assumption of a state-independent effective charge. The corresponding predictions for the $\frac{3}{2}^-(2.63)\rightarrow\frac{7}{2}^-$(g.s.) transition differ far more seriously as a result of destructive interference between the matrix elements of the proton and neutron $E2$ operators. A measurement of the lifetime of either of these states would be helpful in interpreting $E2$ transitions in this nucleus.

We should like to thank Miss F. Darema for help in the early stages of this calculation.

---

*Work performed under the auspices of the United States Atomic Energy Commission.

[1]R. L. Place, K. H. Buerger, Jr., T. Wakatsuki, and B. D. Kern, Phys. Rev. C 3, 2259 (1971).

[2]S. H. Henson, S. Cochavi, D. B. Fossan, and J. D. Vergados, Phys. Rev. C **5**, 791 (1972).

[3]J. L. Yntema, private communication.

[4]F. Ajzenberg-Selove, J. D. Garrett, and O. Hansen, to be published.

[5]J. G. Pronko and R. E. McDonald, Phys. Rev. C 7, 1061 (1973).

[6]S. Maripuu and G. A. Hokken, Nucl. Phys. **A141**, 481 (1970).

[7]A. D. Jackson, T. T. S. Kuo, and J. D. Vergados, Phys. Lett. **30B**, 455 (1969).

[8]H. P. Jolly and L. B. Hubbard, Phys. Rev. C **1**, 1979 (1970).

[9]Y. Shadmi and I. Talmi, Phys. Rev. **129**, 1286 (1963).

[10]J. B. McGrory and B. H. Wildenthal, Phys. Lett. **28**, 237 (1968).

[11]R. D. Lawson, Nucl. Phys. **A173**, 17 (1971).

[12]R. K. Bansal and J. B. French, Phys. Lett. **11**, 145 (1964).

[13]A. H. Wapstra and N. B. Gove, Nucl. Data **A9**, 267 (1971).

[14]J. D. Garrett, private communication.

[15]P. M. Endt and C. van der Leun, Nucl. Phys. **A105**, 1 (1967).

[16]J. B. McGrory, B. H. Wildenthal, and E. C. Halbert, Phys. Rev. C **2**, 186 (1970).

[17]P. Federman and I. Talmi, Phys. Lett. **22**, 469 (1966).

[18]R. M. Freeman and A. Gallmann, Nucl. Phys. **A156**, 305 (1970).
[19]D. Kurath and R. D. Lawson, Phys. Rev. C **6**, 901 (1972).
[20]P. W. M. Glaudemans, B. H. Wildenthal, and J. B. McGrory, Phys. Lett. **21**, 427 (1966).
[21]G. A. P. Engelbertink and G. van Middelkop, Nucl. Phys. **A138**, 588 (1969).
[22]A. N. James, P. R. Aldeson, D. C. Bailey, P. E. Carr, J. L. Durell, L. L. Green, M. W. Greene, and J. F. Sharpey-Schafer, Nucl. Phys. **A168**, 56 (1971).
[23]C. W. Towsley, D. Cline, and R. N. Horoshko, Phys. Rev. Lett. **28**, 368 (1972).
[24]W. Fitz, R. Jahr, and R. Santo, Nucl. Phys. **A114**, 392 (1968).
[25]R. Bass and F. M. Saleh-Bass, Nucl. Phys. **A95**, 38 (1967).
[26]S. A. Moszkowski, in *Alpha-, Beta-, and Gamma-Ray Spectroscopy*, edited by K. Siegbahn (North-Holland, Amsterdam, 1965), Vol. 2, p. 863.
[27]D. Kurath and R. D. Lawson, Phys. Rev. **161**, 915 (1967).
[28]G. A. P. Engelbertink, E. K. Warburton, and J. W. Olness, Phys. Rev. C **5**, 128 (1972).
[29]D. B. Fossan and A. R. Poletti, Phys. Rev. **152**, 984 (1966); Phys. Lett. **24B**, 38 (1967).
[30]R. D. Lawson and M. H. Macfarlane, Nucl. Phys. **66**, 80 (1965).
[31]O. Skeppstedt, R. Hardell, and S. E. Arnell, Ark. Fys. **35**, 527 (1967).
[32]R. Hardell and C. Beer, Phys. Scr. **1**, 85 (1970).
[33]M. Bini, P. G. Bizzeti, A. M. Bizzeti-Sona, R. A. Ricci, Phys. Rev. C **6**, 784 (1972).
[34]I. Talmi, Phys. Rev. **126**, 1096 (1962).

PHYSICAL REVIEW C VOLUME 7, NUMBER 5 MAY 1973

Slow-Neutron Scattering by a Standing Electromagnetic Wave

C. Stassis
Ames Laboratory – U. S. Atomic Energy Commission and Department of Physics, Iowa State University, Ames, Iowa 50010
(Received 3 August 1972)

We examine the elastic scattering of slow neutrons by a standing electromagnetic wave. It is shown that the real part of the coherent scattering amplitude arises essentially from the interaction of the induced electric dipole moment in the neutron with the electric field of the wave. The imaginary part of the coherent scattering amplitude arises from the interference between the magnetic dipole and spin-orbit interaction terms.

I. INTRODUCTION

The advent of lasers has motivated a considerable amount of theoretical work on the interaction of the radiation field with photons and free electrons.[1] The particular focus of interest has been on the possible existence of nonlinear effects[2] in familiar quantum processes such as Compton scattering. The photon densities required for the experimental observation of these effects is of the order of 10^{27} photons/cm^3 at optical frequencies. In considering the scattering of particles by a photon beam of such high density the polarization of the particle by the radiation electric field should be taken into account. In the scattering of a charged particle the contribution to the scattering cross section of the interaction of the induced electric dipole moment in the particle with the electric field is insignificant, compared to that arising from the coupling of the charge of the particle to the electric field. In the case of a neutral particle, on the other hand, the latter term is absent and the contribution to the scattering cross section of the induced electric dipole interaction term may be of importance. The main interest of such scattering experiments would come from the possibility of obtaining information about the polarizability of the particle. In the present paper we examine, in some detail, the scattering of long-wavelength neutrons by the field of an electromagnetic wave.

The main physical aspects of the problem may be qualitatively understood by examining the interaction of a neutron with the electromagnetic field of the wave. The static electric dipole moment of the neutron has been experimentally found to be zero to high accuracy,[3] as required by parity and time-reversal invariance in electromagnetic interactions.[4] However, when a neutron encounters an electromagnetic wave an electric dipole moment $\vec{d} = \alpha \vec{E}$ will be induced in the neutron by the electric field $\vec{E}$ of the wave, if its electric polarizability α has a finite nonzero value.[5] The interaction, $-\frac{1}{2}\alpha \vec{E}^2$, of this induced neutron electric dipole moment with the electric field will contribute to the neutron elastic scattering cross section, in the first order of perturbation theory. In addition the neutron possesses a magnetic moment μ of $-1.91\mu_N$ which couples to the electromagnetic field through the well-known magnetic dipole[6] and spin-orbit interaction term.[7] Both these terms will contribute, in the